

The Influence of Side-Chain Halogenation on the Self-Assembly and Hydrogelation of Fmoc-Phenylalanine Derivatives

Derek M. Ryan, Samuel B. Anderson, and Bradley L. Nilsson*

Department of Chemistry, University of Rochester, Rochester, NY, 14627

ELECTRONIC SUPPORTING INFORMATION

Contents:

Figure S1 SEM images of Fmoc-n-X-Phe derivatives.....	page 1
Table S1 Tabulation of CD absorptions for each Fmoc-n-X-Phe derived hydrogel.....	page 2
Figure S2 Empirical curve fit of Fmoc-2-F-Phe kinetics.....	page 3
Figure S3 Empirical curve fit of Fmoc-2-Cl-Phe kinetics.....	page 4
Figure S4 Empirical curve fit of Fmoc-2-Br-Phe kinetics.....	page 4
Figure S5 Empirical curve fit of Fmoc-3-F-Phe kinetics.....	page 5
Figure S6 Empirical curve fit of Fmoc-3-Cl-Phe kinetics.....	page 5
Figure S7 Empirical curve fit of Fmoc-3-Br-Phe kinetics.....	page 6
Figure S8 Empirical curve fit of Fmoc-4-F-Phe kinetics.....	page 7
Figure S9 Empirical curve fit of Fmoc-4-Cl-Phe kinetics.....	page 7
Figure S10 Empirical curve fit of Fmoc-4-Br-Phe kinetics.....	page 8
Figure S11 UV-Vis absorbance spectra of Fmoc-X-F-Phe monomers and hydrogels.....	page 9
Figure S12 UV-Vis absorbance spectra of Fmoc-X-Cl-Phe monomers and hydrogels.....	page 9
Figure S13 UV-Vis absorbance spectra of Fmoc-X-Br-Phe monomers and hydrogels.....	page 9
Figure S14 Fluorescence emission spectra of Fmoc-X-F-Phe monomers and hydrogels...page 10	page 10
Figure S15 Fluorescence emission spectra of Fmoc-X-Cl-Phe monomers and hydrogels..page 10	page 10
Figure S16 Fluorescence emission spectra of Fmoc-X-Br-Phe monomers and hydrogels..page 10	page 10

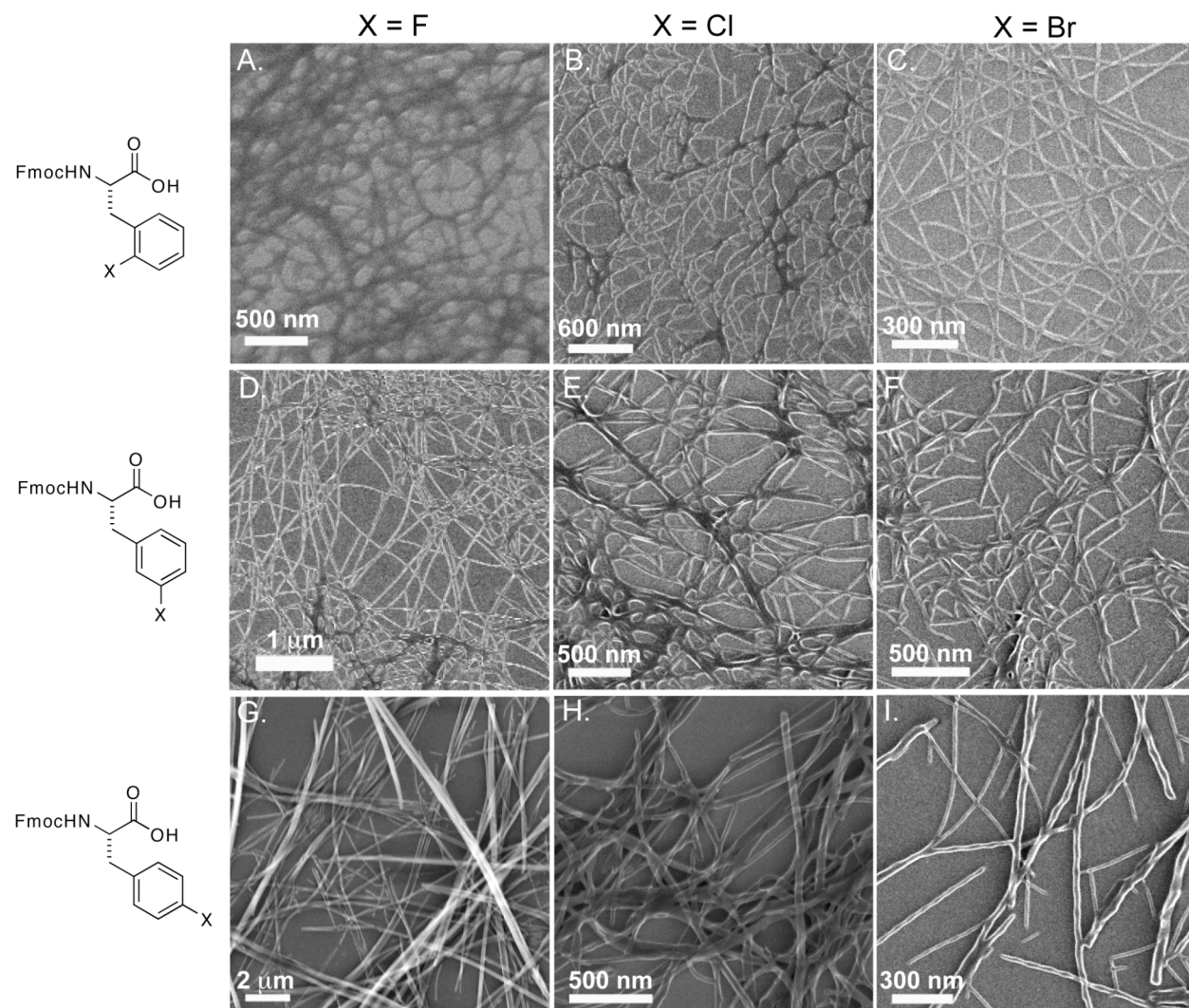


Figure S1. SEM images of Fmoc-n-X-Phe amino acids after a 3 day maturation period. A) Fmoc-2-F-Phe; B) Fmoc-2-Cl-Phe; C) Fmoc-2-Br-Phe; D) Fmoc-3-F-Phe; E) Fmoc-3-Cl-Phe; F) Fmoc-3-Br-Phe; G) Fmoc-4-F-Phe; H) Fmoc-4-Cl-Phe; I) Fmoc-4-Br-Phe.

Table S1. Tabulation of CD absorptions for each Fmoc-n-X-Phe derived hydrogel (min = minimum, max = maximum).

Amino acid	Major absorptions (nm)
Fmoc-2-F-Phe	200 (min), 224 (max), 275 (max), 293 (max), 307 (max)
Fmoc-2-Cl-Phe	207 (min), 225 (max), 278 (max), 296 (max), 307 (max)
Fmoc-2-Br-Phe	211 (min), 268 (min), 294 (min), 307 (min)
Fmoc-3-F-Phe	201 (min), 220 (max), 274 (max), 295 (max), 307 (max)
Fmoc-3-Cl-Phe	207 (min), 226 (max), 276 (max), 295 (max), 307 (max)
Fmoc-3-Br-Phe	210 (min), 228 (max), 279 (max), 296 (max), 309 (max)
Fmoc-4-F-Phe	229 (min), 289 (min), 298 (min), 310 (min)
Fmoc-4-Cl-Phe	209 (min), 231 (min), 279 (min), 296 (min), 309 (min)
Fmoc-4-Br-Phe	213 (min), 232 (max), 284 (max), 296 (max), 309 (max)

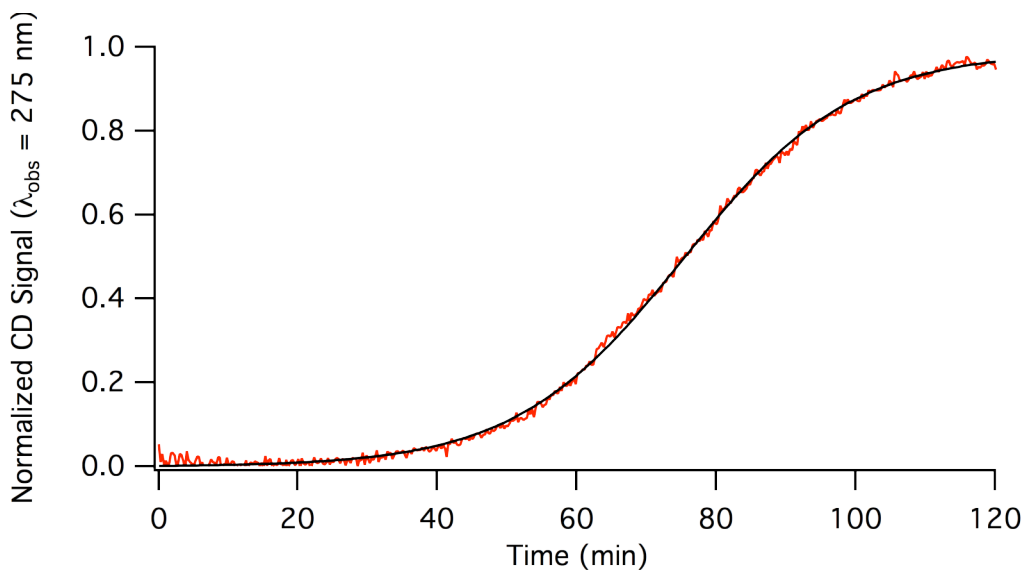


Figure S2. Representative empirical curve fit for Fmoc-2-F-Phe self-assembly kinetics ($t_{1/2} = 75 \pm 5 \text{ min}$, $k = 0.08 \pm 0.02 \text{ min}^{-1}$).

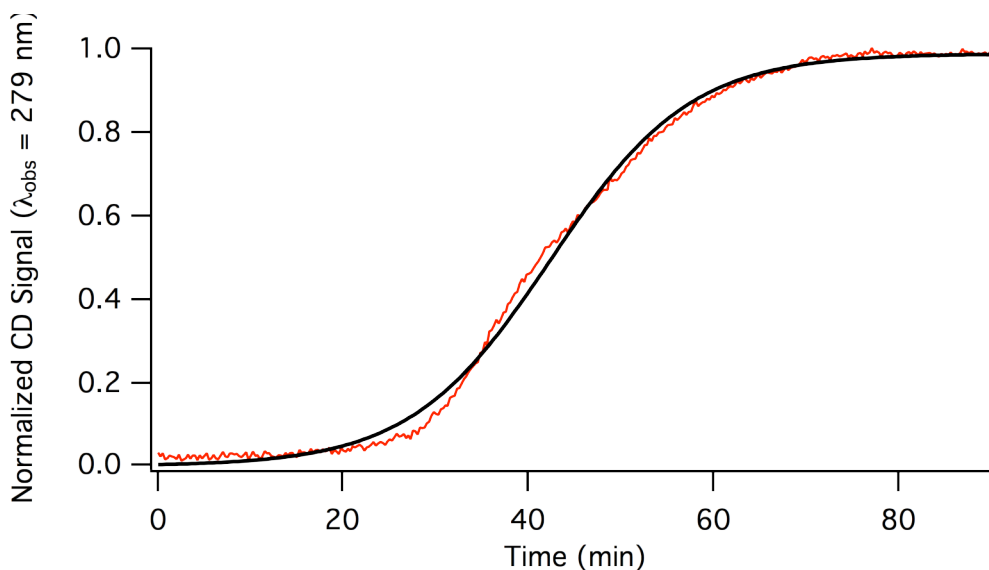


Figure S3. Representative empirical curve fit for Fmoc-2-Cl-Phe self-assembly kinetics ($t_{1/2} = 41 \pm 4 \text{ min}$, $k = 0.2 \pm 0.1 \text{ min}^{-1}$).

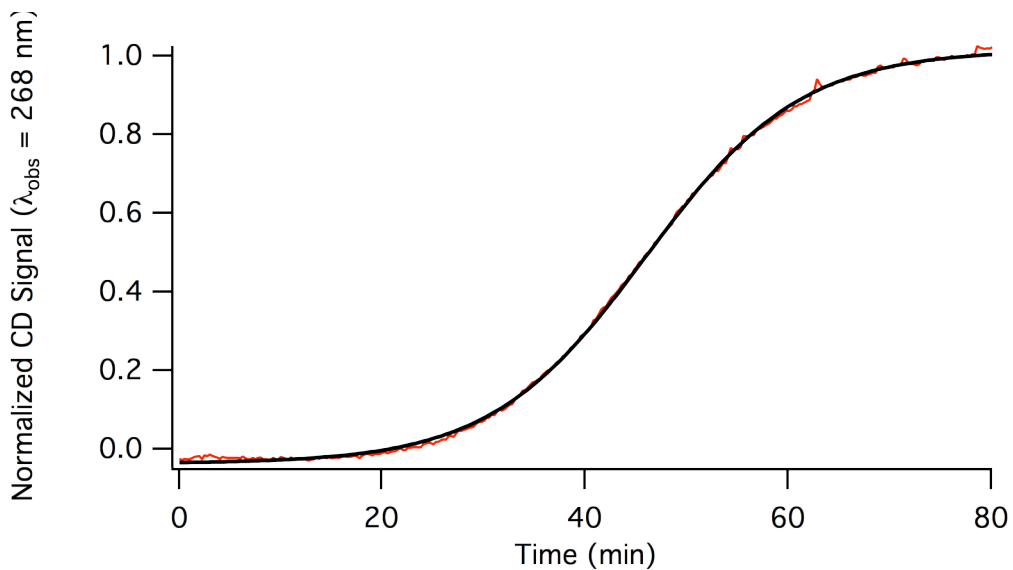


Figure S4. Representative empirical curve fit for Fmoc-2-Br-Phe self-assembly kinetics ($t_{1/2} = 47 \pm 3 \text{ min}$, $k = 0.12 \pm 0.03 \text{ min}^{-1}$).

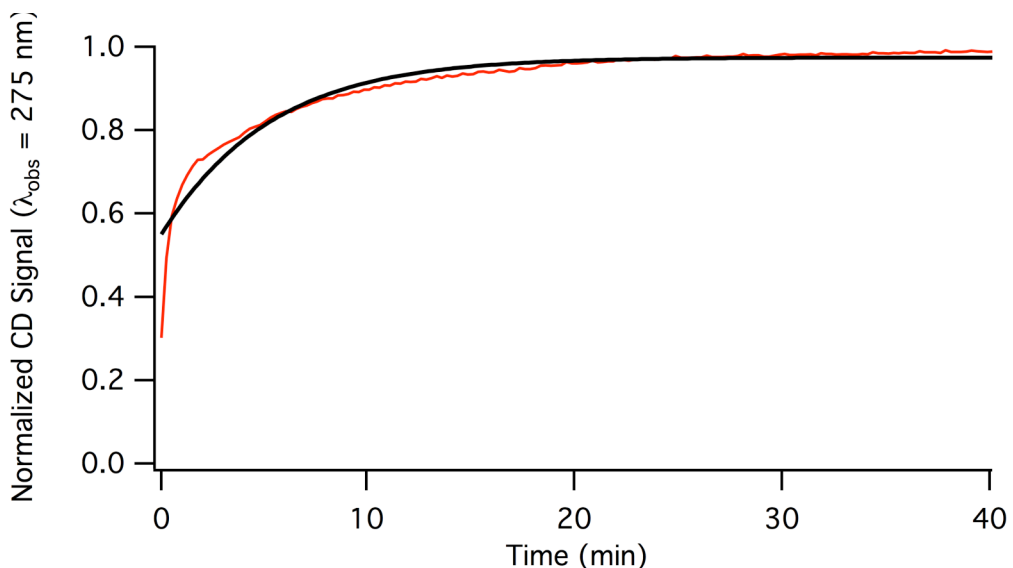


Figure S5. Representative empirical curve fit for Fmoc-3-F-Phe self-assembly kinetics (reliable $t_{1/2}$ and k values could not be obtained due to the lack of an observable lag phase).

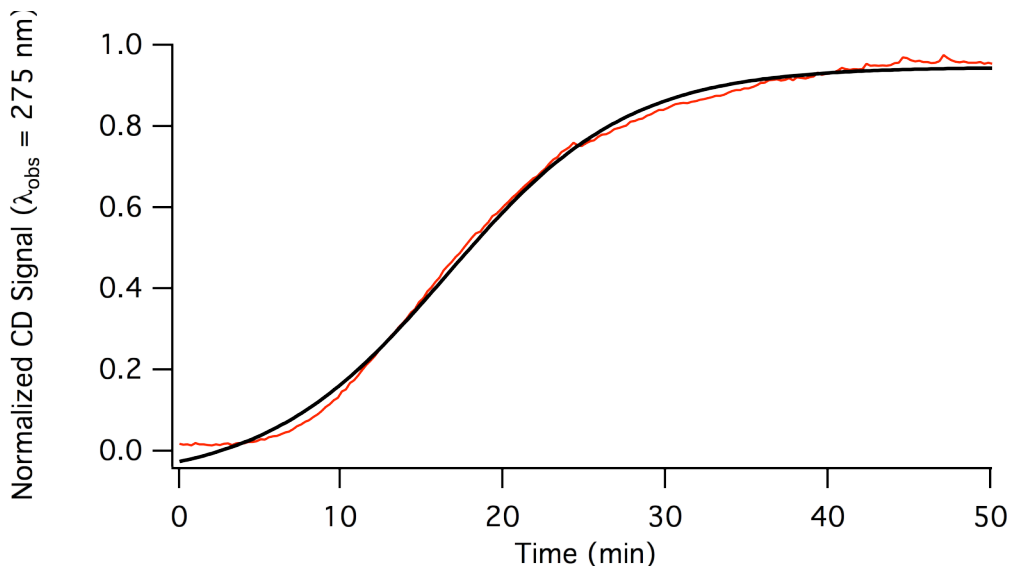


Figure S6. Representative empirical curve fit for Fmoc-3-Cl-Phe self-assembly kinetics ($t_{1/2} = 18 \pm 2 \text{ min}$, $k = 0.23 \pm 0.03 \text{ min}^{-1}$).

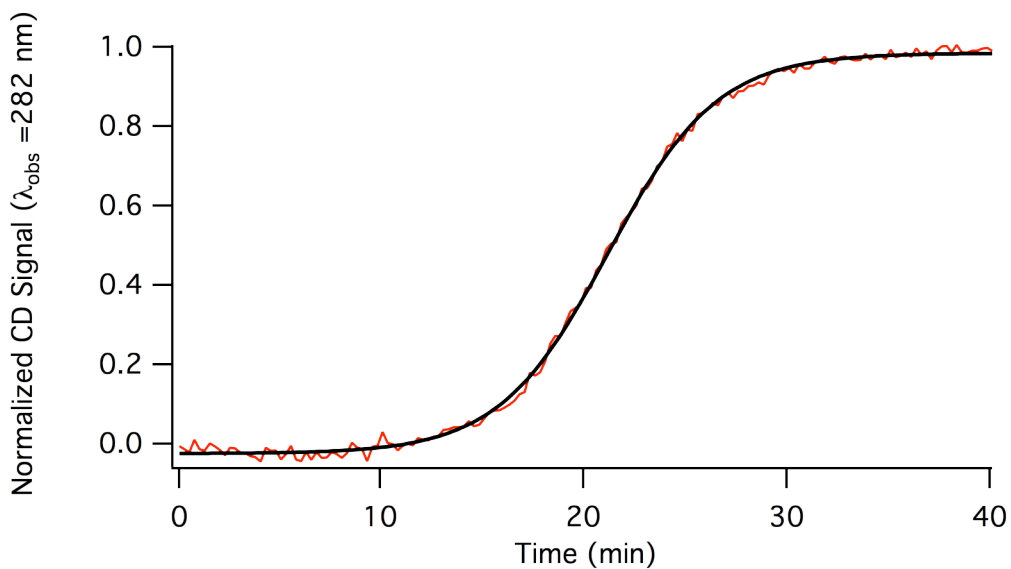


Figure S7. Representative empirical curve fit for Fmoc-3-Br-Phe self-assembly kinetics ($t_{1/2} = 21 \pm 1 \text{ min}$, $k = 0.6 \pm 0.3 \text{ min}^{-1}$).

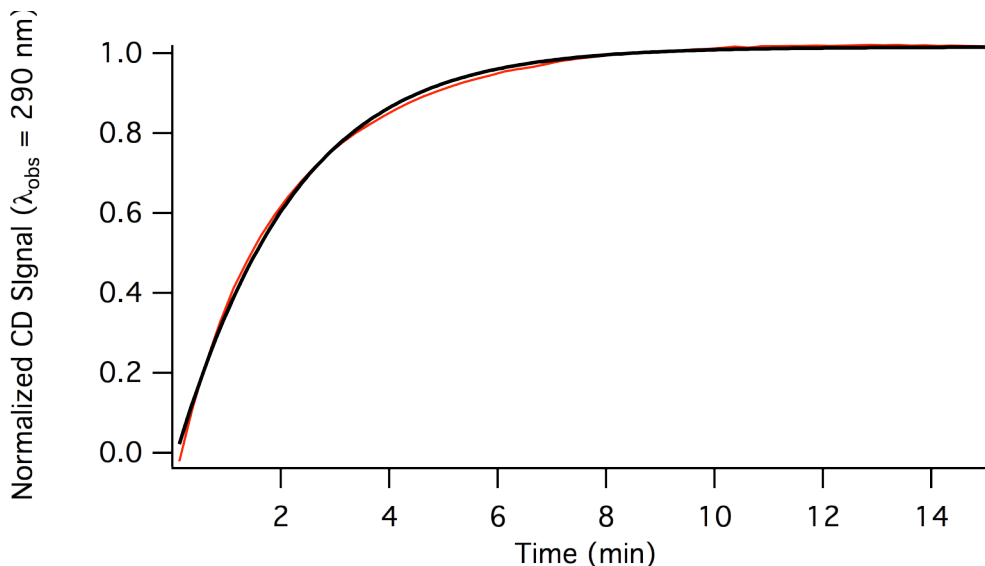


Figure S8. Representative empirical curve fit for Fmoc-4-F-Phe self-assembly kinetics (reliable $t_{1/2}$ and k values could not be obtained to the lack of an observable lag phase).

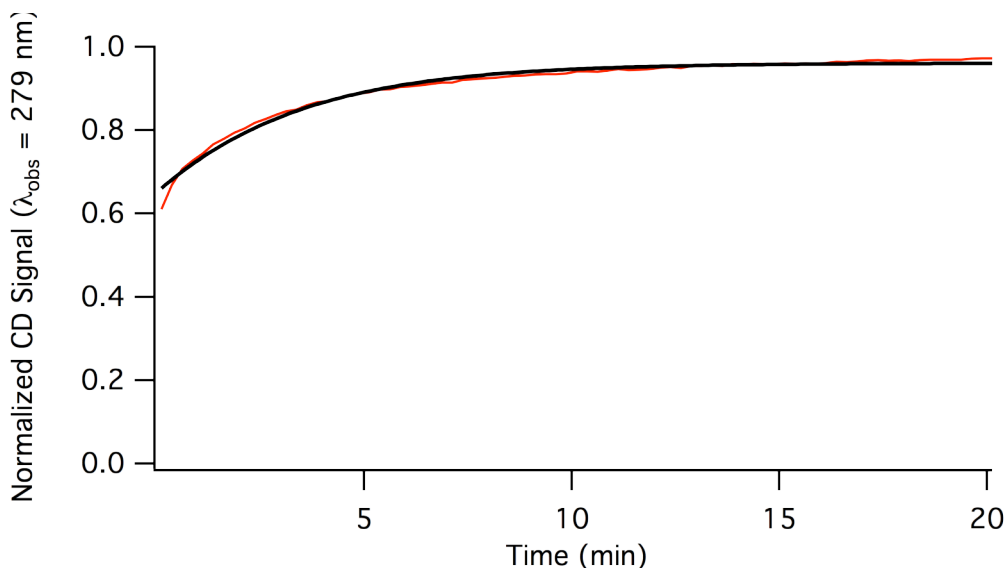


Figure S9. Representative empirical curve fit for Fmoc-4-Cl-Phe self-assembly kinetics (reliable $t_{1/2}$ and k values could not be obtained to the lack of an observable lag phase).

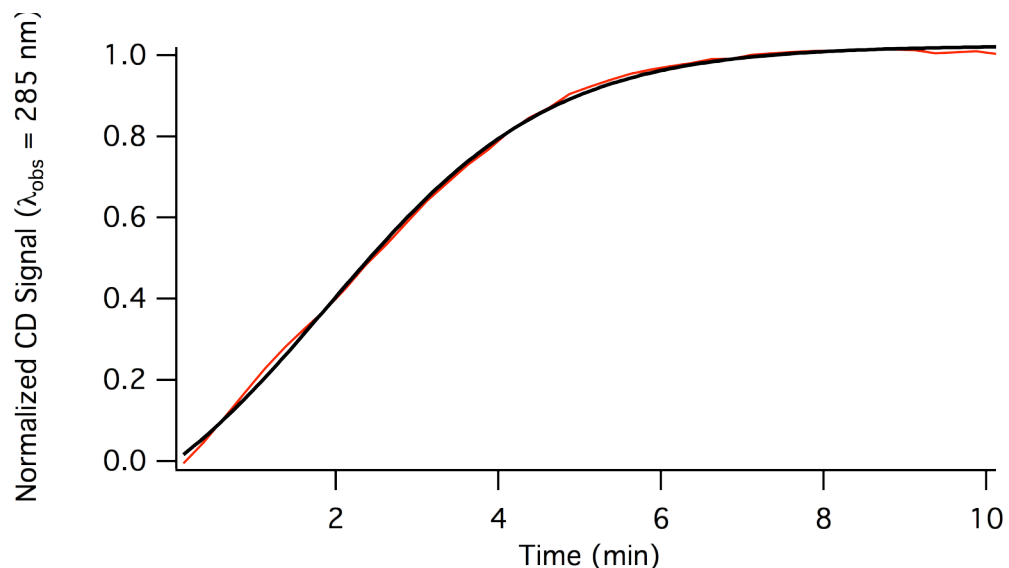


Figure S10. Representative empirical curve fit for Fmoc-4-Br-Phe self-assembly kinetics (reliable $t_{1/2}$ and k values could not be obtained due to the lack of an observable lag phase).

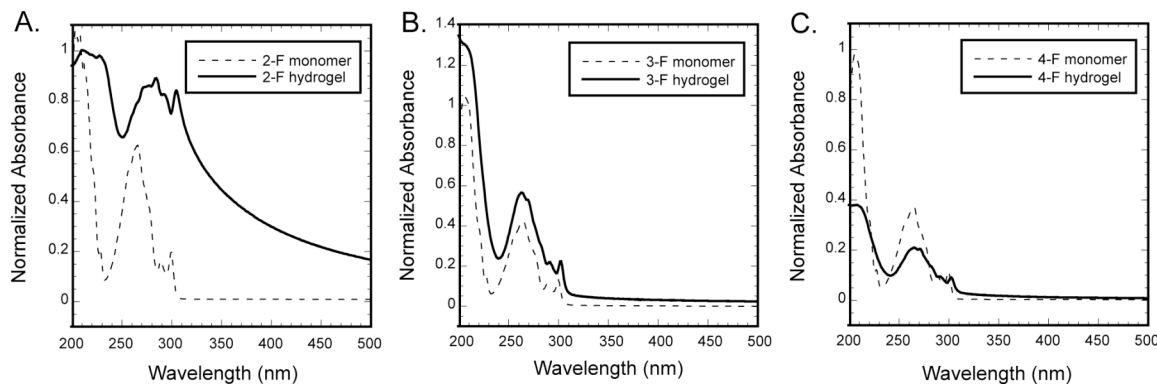


Figure S11. Normalized UV-Vis absorbance of monomeric Fmoc-n-F-Phe derivatives (4.94 mM in MeOH) and assembled Fmoc-n-F-Phe derivatives (4.94 mM in 2% MeOH/H₂O). A) Fmoc-2-F-Phe; B) Fmoc-3-F-Phe; C) Fmoc-3-Cl-Phe.

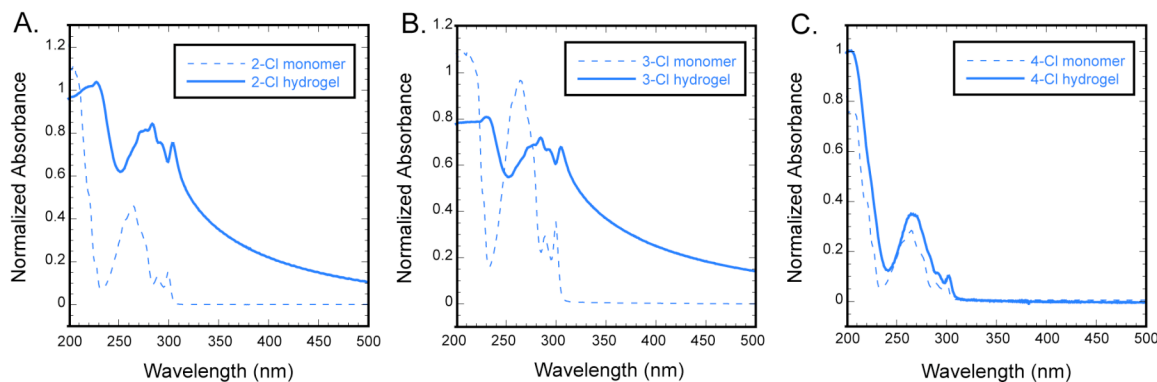


Figure S12. Normalized UV-Vis absorbance of monomeric Fmoc-n-Cl-Phe derivatives (4.94 mM in MeOH) and assembled Fmoc-n-Cl-Phe derivatives (4.94 mM in 2% MeOH/H₂O). A) Fmoc-2-Cl-Phe; B) Fmoc-3-Cl-Phe; C) Fmoc-4-Cl-Phe.

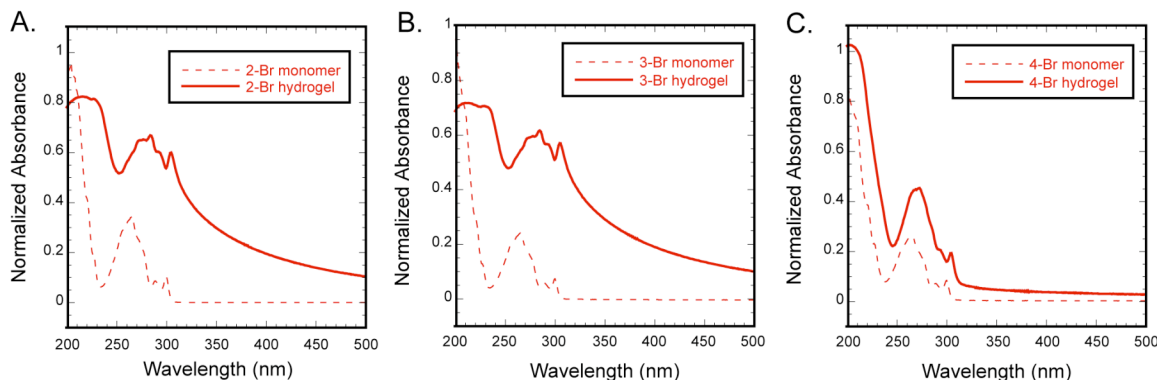


Figure S13. Normalized UV-Vis absorbance of monomeric Fmoc-n-Br-Phe derivatives (4.94 mM in MeOH) and assembled Fmoc-n-Br-Phe derivatives (4.94 mM in 2% MeOH/H₂O). A) Fmoc-2-Br-Phe; B) Fmoc-3-Br-Phe; C) Fmoc-4-Br-Phe.

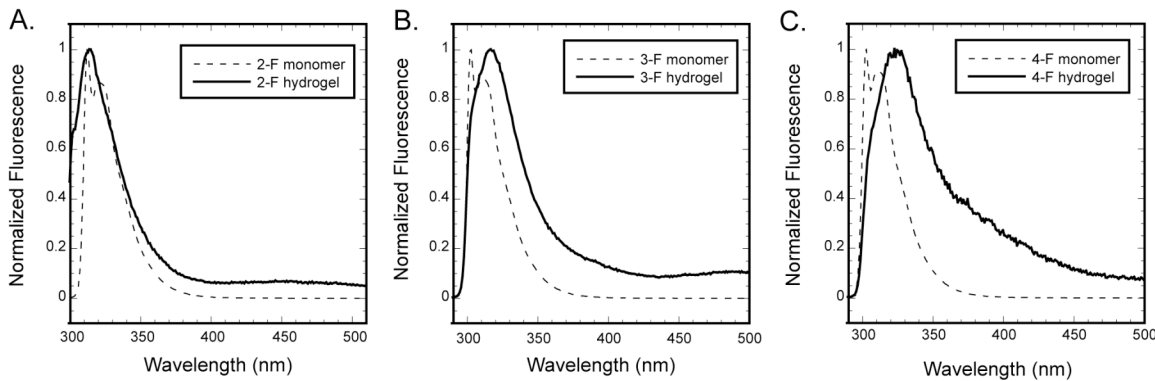


Figure S14. Normalized fluorescence emission spectra of monomeric Fmoc-n-Br-Phe derivatives (4.94 mM in MeOH) and assembled Fmoc-X-Br-Phe derivatives (4.94 mM in 2% MeOH/H₂O). A) Fmoc-2-Br-Phe; B) Fmoc-3-Br-Phe; C) Fmoc-4-Br-Phe.

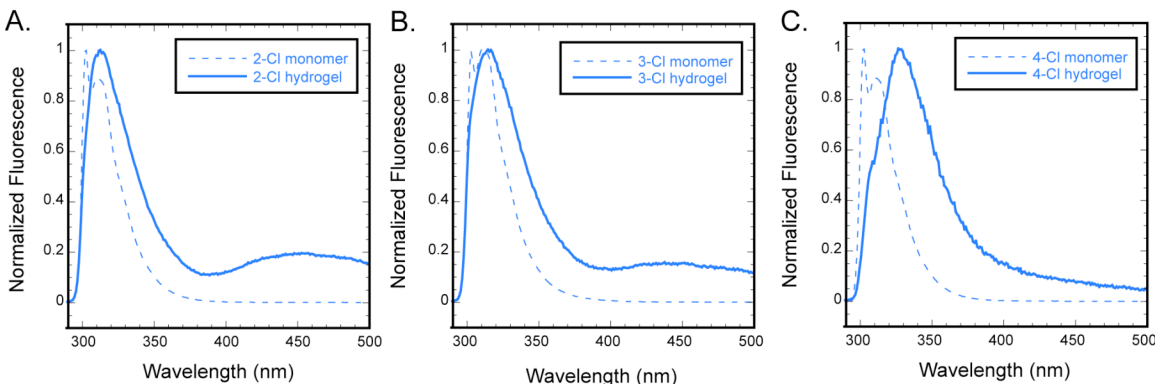


Figure S15. Normalized fluorescence emission spectra of monomeric Fmoc-n-Br-Phe derivatives (4.94 mM in MeOH) and assembled Fmoc-n-Br-Phe derivatives (4.94 mM in 2% MeOH/H₂O). A) Fmoc-2-Br-Phe; B) Fmoc-3-Br-Phe; C) Fmoc-4-Br-Phe.

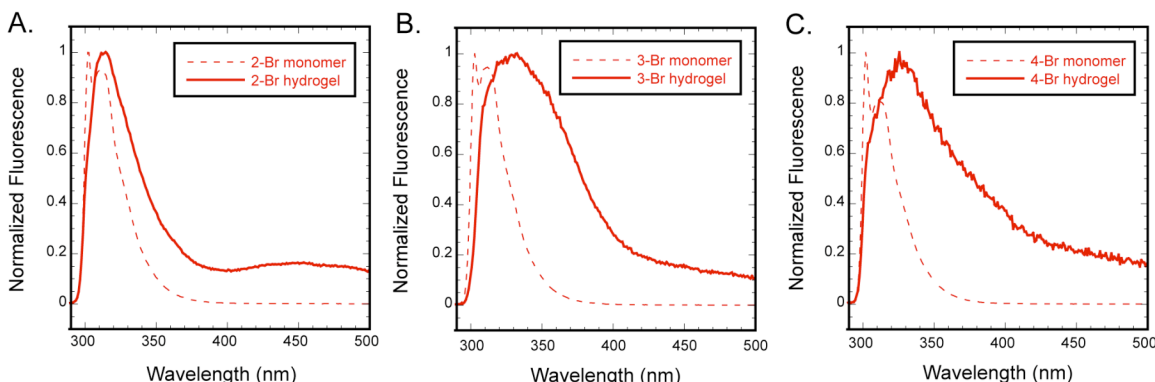


Figure S16. Normalized fluorescence emission spectra of monomeric Fmoc-n-Br-Phe derivatives (4.94 mM in MeOH) and assembled Fmoc-n-Br-Phe derivatives (4.94 mM in 2% MeOH/H₂O). A) Fmoc-2-Br-Phe; B) Fmoc-3-Br-Phe; C) Fmoc-4-Br-Phe.